Performance of Coded Single-Band Carrier-Based DS-SS Systems on IEEE 802.15.3a UWB Channels

Matts-Ola Wessman, Arne Svensson, and Erik Agrell
Communication System Group, Department of Signals and Systems,
Chalmers University of Technology, SE-412 96 Gothenburg, Sweden
Email: {mow, arnes, agrell}@chalmers.se

***Abstract*— A set of physical layer specifications is provided for a single-band system. The system fulfills the FCC regulations on UWB devices and the physical layer requirements from IEEE 802.15.3a. It gives reliable communication, i.e., a 90th-percentile PER equal to 8% for 1024 payload bytes, at 110 Mbps with a transmitter–receiver separation of up to 10 meters on the IEEE 802.15.3a channel model CM4. 205 Mbps at 6.7 meters on CM4 and 513 Mbps at 3.8 meters on CM2 are also achieved. The system uses the spectrum 3.1–4.9 GHz, a chip-spaced rake combiner with 60 fingers, a sliding window channel estimator, and a sampling rate of 1540 Msamples/s.**

I. Introduction

In the near future, there will appear a demand for low cost, high-speed, wireless links for short range (< 10 m) communication. Ultra-wideband (UWB) systems could provide those features. UWB systems can be classified to be either single band or multiband and to use either carrier based radio or impulse radio. FCC restricted that UWB devices have to use at least 500 MHz instantaneous bandwidth in the 3.1–10.6 GHz band with a power spectral density of at most –41.25 dBm/MHz [1]. This leads to very low transmit power.

Within the IEEE 802.15 working group for wireless personal area network (WPAN), the standardization of an alternative, high rate, physical layer, denoted 802.15.3a, is ongoing. The result after the down selection of several proposals are two merged proposals. The first is denoted multiband-OFDM (MB-OFDM) and the second is denoted DS-UWB [2]–[5]. The DS-UWB system uses two bands with BPSK or quaternary biorthogonal keying (4BOK). A new UWB channel model based on the Saleh–Valenzuela model was adopted and used in the evaluation of the several physical layer proposals [6], [7].

In parallel to the 802.15.3a standardization, the EU research project Ultrawaves investigated UWB from, e.g, physical layer, MAC layer, antennas, and channel modeling points of view. Coherent and noncoherent impulse radio systems with 100 Mbps and repetition codes were compared on the IEEE 802.15.3a channel model. Both systems used higher-order derivatives of the Gaussian pulse in order to comply with the FCC regulations. The physical layer was decided to be a coherent, single-band system using up- and down-converters. See [8]–[11] for details.

The main objective of this paper is to find the system specification for a single-band, coherent, carrier-based direct-sequence spread-spectrum (DS-SS) system that fulfills the physical layer requirements from IEEE 802.15.3a. Based on [6], [12], [13], the investigated system should provide at least a payload bit rate of 110 Mbps at 10 meters and at least 200 Mbps at 4 meters. An optional requirement is at least 480 Mbps at 2 meters. The packet error rate (PER) should be less than or equal to 8% for a payload of 1024 information bytes per packet. Additional results on a dual-band system using a fractionally-spaced receiver can be found in [14].

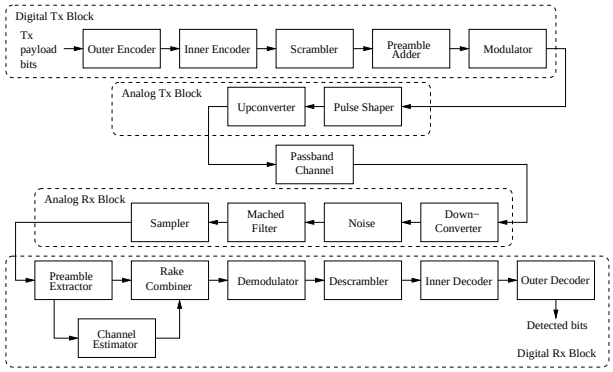

Fig. 1. The system model of the investigated system.

II. System Model

Fig. 1 depicts the system model that consists of a digital transmitter block, an analog transmitter block, a channel, an analog receiver block, and a digital receiver block.

A. Transmitter–Receiver Algorithms

1) Digital Transmitter Block: The digital transmitter encodes first N_i information bits per packet using an outer convolutional code with rate $k_{\text{CC}}/n_{\text{CC}}$ and an inner repetition code with rate $1/n_{\text{rep}}$. Then the encoded bits are scrambled. The outer encoder, the inner encoder, and the scrambler create a DS-SS signal, which is defined here to be the payload of a packet. Then N_p known pseudo-white pilots are added as a preamble before the payload. Finally, complex-valued chips are generated by quadrature modulating the signal with $\log_2 M$ bits per chip, where M is the constellation size.

The concatenated code has code rate k/n, where $k = k_{\text{CC}}$ and $n = n_{\text{CC}} n_{\text{rep}}$. The number of payload chips and pilot chips per packet are $N_i n/(k \log_2 M)$ and $N_p/\log_2 M$, respectively. If R_c is the chip rate, then the payload bit rate is given by $R_b = kR_c \log_2 M/n$. The duration of one chip is $T_c = 1/R_c$.

2) Analog Transmitter and Receiver Blocks: In the analog transmitter block, the complex modulated chips from the digital transmitter block are pulse shaped and upconverted to carrier frequency f_c. In the analog receiver block, the passband signal from the channel is downconverted to baseband. Complex front end receiver noise is added, before the signal is pulse-matched filtered. Finally, the signal is sampled with a sampling time T_{samp}.

3) Digital Receiver Block: The digital receiver has a preamble extractor, a channel estimator, a rake combiner, a demodulator, a descrambler, an inner decoder, and an outer decoder. After finding the preamble, the channel estimator estimates the complex baseband representation of the impulse response of the passband channel with a sliding window (SW) algorithm. The estimator cross-correlates the received pilot sequence and the transmitted pilot sequence. Then it finds the N_R complex-valued gains $\{\hat{a}_l\}$ and delays $\{\hat{\tau}_l\}$ that correspond to the N_R largest amplitudes of the cross-correlated sequence. Each delay $\hat{\tau}_l$ is an integer times the sampling time T_{samp}.

A selective rake combiner is used to equalize the received payload. The signals in the N_R strongest rake fingers are combined in a maximum ratio fashion (MRC). The equalized signal is then demodulated into a real-valued stream and descrambled. The inner repetition decoder is a soft-input soft-output decoder, which adds up the received amplitudes corresponding to n_{rep} coded bits. The outer Viterbi decoder uses soft-decision decoding.

B. Channel Models

1) Free Space Channel or the AWGN Channel: A flat, time-static channel with free space propagation loss and only additive white gaussian noise (AWGN) is here referred to as the AWGN channel or the free space channel. The impulse response $h(t) = \delta(t)$. A channel impulse response (CIR) gain G_{CIR} is defined to be given by $G_{\text{CIR}} = \int_0^\infty |V(f - f_c)H(f)|^2 \, df$, where $V(f)$ is the continuous-time Fourier transform (CTFT) of the transmitted waveform that is normalized so that $\int_{-\infty}^{\infty} |V(f)|^2 \, df = 1$. Further, f_c is the carrier frequency and $H(f)$ is the CTFT of $h(t)$. This definition does not consider the free space path loss. For the AWGN channel, G_{CIR} is always one. Assume that the waveform can be approximated with a brick-wall filter with bandwidth B, then the gain can be approximated with

$$G_{\text{CIR}} \approx \frac{1}{B} \int_{f_c - B/2}^{f_c + B/2} |H(f)|^2 \, df. \tag{1}$$

2) IEEE 802.15.3a Channel Model: The IEEE 802.15.3a channel model is a stochastic channel model, where a new channel impulse response $h(t)$ is drawn for every connection. Each CIR, i.e, each realization of the channel model, is generated independently from previously generated CIRs. The G_{CIR} is here a random variable.

The IEEE 802.15.3a channel model is based on the Saleh–Valenzuela model where multipath components arrive in clusters [6], [7]. This multipath channel can be expressed as

$$h(t) = Xc(t) = \frac{X}{\sqrt{G_\alpha}} \sum_{l=0}^{\infty} \sum_{k=0}^{\infty} \alpha_{k,l} \delta(t - T_l - \tau_{k,l}), \tag{2}$$

where the real-valued multipath gain is defined by $\alpha_{k,l}$ for cluster l and ray k. The lth cluster arrives at T_l and its kth ray arrives at $\tau_{k,l}$, which is relative to the first path in cluster l, i.e., $\tau_{0,l} = 0$. X denotes log-normal shadowing. Further, $G_\alpha = \sum_{k,l} |\alpha_{k,l}|^2$.

The random variables $\{\alpha_{k,l}\}$ are generated independently but are not identically distributed. The expected value $\mathrm{E}[|\alpha_{k,l}|^2]$ is proportional to $\exp(-T_l/\Gamma - \tau_{k,l}/\gamma)$, where Γ and γ denote a cluster- and a ray-decay factor, respectively. The amplitude $|\alpha_{k,l}|$ has a log-normal distribution since the clusters and the rays fade with two independent log-normally distributed random variables. Further, the phase $\angle\alpha_{k,l}$ is chosen from $\{0, \pi\}$ with equal probability. The log-normal shadowing is modeled with $X = 10^{n/20}$, where n has a normal distribution with mean $\mu_n = 0$ and standard deviation $\sigma_n = 3$.

The arrival times of the clusters and the rays within one cluster are given by two independent Poisson processes with intensities Λ and λ, respectively. The arrival time of the first cluster T_0 is zero for line-of-sight (LOS) models and exponentially distributed with intensity Λ for nonline-of-sight (NLOS) models. Tab. I gives some data for the four models CM1, CM2, CM3, and CM4. See [6] for a more detailed explanation of the models and the values of, e.g., $\Lambda, \lambda, \Gamma, \gamma$.

TABLE I
THE 802.15.3A CHANNEL MODEL

	CM1	CM2	CM3	CM4	unit
Tx–Rx separation	0–4	0–4	4–10		m
(Non-)line of sight	LOS	NLOS	NLOS	NLOS	
Mean excess delay	5.0	9.9	15.9	30.1	ns
RMS delay	5	8	15	25	ns

C. Link Budget and Energy per Bit

There are two important outputs from a link budget, an Rx sensitivity Ψ and a link margin M_L. Also, the budget connects an energy per bit to a distance. The link budget here is adapted from [6] but, e.g, the G_{CIR} and a processing gain PG have been added. Let d be the transmitter–receiver (T–R) separation in meters. Then the received power is

$$P_r = P_{r,\text{fs}} G_{\text{CIR}} = \frac{P_t G_t G_r}{L_p(d)} G_{\text{CIR}}, \tag{3}$$

where $P_{r,\text{fs}}$ is the received power and G_{CIR} is the channel impulse response gain. Further, P_t is the average transmitted power, G_t is the transmitter antenna gain, and G_r is the receiver antenna gain. The power $P_{r,\text{fs}}$ is assumed to be given by the Friis free-space transmission equation with one modification. The path loss is given here by $L_p(d) = (4\pi d f_c'/c)^2$, where c is the speed of light and $f_c' = \sqrt{f_{\text{min}} f_{\text{max}}}$, where f_{min}

and $f_{\max}$ are the -10 dB edges of the pulseform spectrum. The path loss coefficient n_{plc} is two.

The total noise power in the receiver is $P_N = N_{0,t} B_N N_F L_I$, where $N_{0,t} = -173.84$ dBm/Hz is the spectral density of the thermal noise, B_N is the noise bandwidth, N_F is the receiver noise figure, and L_I is the implementation loss. Further, the thermal noise power is $N_t = N_{0,t} B_N$ and the spectral density of the noise after despreading is $N_0 = N_{0,t} N_F L_I$. The implementation loss is the loss due to hardware impairments such as filter distortion, phase noise, quantization noise, and frequency errors that occur on the AWGN channel.

The received signal-to-noise ratio per payload bit, ε_{pb}/N_0, is defined to consider only the effects of coding and modulation, and to ignore the energy loss due to any preamble. Let $P_r = \varepsilon_{pb} R_b$ and the processing gain $\text{PG} = B_N/R_b$. Then $\varepsilon_{pb}/N_0 = P_r \text{PG}/P_N = P_{r,\text{fs}} G_{\text{CIR}} \text{PG}/P_N$. Assuming that the noise bandwidth is equal to the chip rate, $B_N = R_c$, leads to $\text{PG} = n/(k \log_2 M)$. The minimum ε_{pb}/N_0 that a system requires to achieve a PER of 8 % on the AWGN channel is denoted Γ_{fs}. It is obtained with ideal hardware and synchronization.

The Rx sensitivity Ψ is the minimum mean received power that is required to give a PER of 8% on the AWGN channel at a certain distance d. The Rx sensitivity is given by $\Psi = \Gamma_{\text{fs}} P_N/\text{PG}$. The mean received power on the AWGN channel is $\bar{P}_{r,\text{AWGN}} = \text{E}[P_r] = P_{r,\text{fs}}$, since $G_{\text{CIR}} = 1$. The link margin is given by $M_L = \bar{P}_{r,\text{AWGN}}/\Psi = P_{r,\text{fs}}/\Psi$. This link margin needs to be large enough so that the system also gives a 90th-percentile PER of 8% on the IEEE 802.15.3a channel models. It covers, e.g., additional implementation losses, imperfect channel estimation, imperfect multipath energy capture, and amplitude fading that occur on CM1–4, which was not considered in L_I.

III. Distribution of the Gain of the CIR

The purpose of this section is to find the distribution of the channel impulse response gain G_{CIR} for the IEEE 802.15.3a channel model. The first step is to find the distribution of $|C(f)|^2$. The CTFT of $h(t)$ in (2) is given by

$$H(f) = XC(f) = X \sum_{l=0}^{\infty} \sum_{k=0}^{\infty} \frac{\alpha_{k,l}}{\sqrt{G_\alpha}} \exp\left(-j2\pi f(T_l + \tau_{k,l})\right), \tag{4}$$

where the definition of $G_\alpha = \sum_{k,l} |\alpha_{k,l}|^2$ is repeated here for clarity. Let m be a bijective function with $m : \mathbb{N}_0^2 \to \mathbb{N}_0$ and let $m = m(k,l)$. Then, $C(f)$ can be rewritten as

$$C(f) = \sum_{m=0}^{\infty} \beta_m \exp\left(-j2\pi f \tau_m\right), \tag{5}$$

where $\beta_m = \alpha_{k,l}/\sqrt{G_\alpha}$ and $\tau_m = T_l + \tau_{k,l}$. The random variables $\{\beta_m\}$ are dependent due to the division with $\sqrt{G_\alpha}$. Since T_l and $\tau_{k,l}$ are generated by independent Poisson processes, the random variables $\{\tau_m\}$ are independent. Also, $\{\tau_m\}$ and $\{\beta_m\}$ are independent. Further, $\{\beta_m \exp(-j2\pi f \tau_m)\}$ are not identically distributed, since the expected value $\text{E}[|\alpha_{k,l}|^2]$ is proportional to $\exp(-T_l/\Gamma - \tau_{k,l}/\gamma)$. Since τ_m is a continuous random variable, $f\tau_m$ is also a continuous random variable. Then there exists a frequency f that is large enough such that the distribution of $\exp(-j2\pi f \tau_m)$ can be approximated with a uniform distribution. Below, only such frequencies are considered. Thus, the random variables $\{\beta_m \exp(-j2\pi f \tau_m)\}$ are uncorrelated.

The central limit theorem requires that the sum of the variances of the random variables goes to infinity when the number of random variables goes to infinity [15]. Thus, the central limit theorem does not hold, since $\sum_{m=0}^{\infty} \text{E}[|\beta_m|^2] < \infty$. However, if the variance of the random variables decays slowly enough, then a large number of random variables with significant variances contribute to the sum of the random variables. Then, it is reasonable to believe that the theorem still applies. If so, for a fixed f that is large enough, $C(f)$ converges in distribution to $C_I(f) + jC_Q(f)$, where $C_I(f)$ and $C_Q(f)$ are normally distributed with zero mean and variance σ^2, where σ^2 is to be determined. Thus, $|C(f)|^2$ is exponentially distributed with mean $2\sigma^2$.

The next step is to determine the variance σ^2. We know that $\text{E}[\exp(-j2\pi f(\tau_m - \tau_n))] = \text{E}[\exp(-j2\pi f \tau_m)]\,\text{E}[\exp(j2\pi f \tau_n)] = 0$ when $m \neq n$. Then we can show that

$$\sigma^2 = \frac{1}{2}\,\text{E}\left[|C(f)|^2\right] = \frac{1}{2} \sum_{m=0}^{\infty} \text{E}\left[|\beta_m|^2\right]. \tag{6}$$

The last step in estimating the distribution of G_{CIR} is started by defining the integral

$$J = \frac{1}{B} \int_{f_c - B/2}^{f_c + B/2} |C(f)|^2 \, df, \tag{7}$$

which leads to $G_{\text{CIR}} \approx X^2 J$. Assume that $|C(f)|^2$ is piecewise constant over a coherence bandwidth B_c. The number of subbands is $N_B = \lfloor B/B_c \rfloor$, where $\lfloor x \rfloor$ denotes the integer part of x. Within each subband, $|C(f)|^2$ is exponentially distributed with mean $2\sigma^2$. The integral J can then be approximated with $J \approx \tilde{J} = \sum_{p=0}^{N_B - 1} J_p/N_B$, where $J_p = |C(f_c - B/2 + B_c(p + 1/2))|$ for $p = 0, \ldots, N_B - 1$ are independent exponentially distributed with mean $2\sigma^2$ and variance $4\sigma^4$. Further, $\{J_p/N_B\}$ have mean $2\sigma^2/N_B$ and variance $4\sigma^4/N_B^2$. Then $\tilde{J}$ has a gamma distribution $\Gamma(q, r)$ with $q = N_B$ degrees of freedom and parameter $r = 1/\,\text{E}[J_p/N_B] = N_B/2\sigma^2$. The mean and variance of $\tilde{J}$ are $2\sigma^2$ and $4\sigma^4/N_B$, respectively.

Thus, the distribution of G_{CIR} can be approximated with a multiplication of two independent random variables, X^2 and $\tilde{J}$, which are log-normally and gamma distributed, respectively, i.e., $G_{\text{CIR}} \approx X^2 \tilde{J}$.

So far, the effect of the division with $\sqrt{G_\alpha}$ in (4) has not been considered in the calculation of $2\sigma^2$. This division gives that $\sum |\beta_m|^2$ is always one for all realizations. Consequently, the variance $\sigma^2 = 1/2$. Moreover, the distributions of $|C(f)|$ and $|H(f)|$ are Rayleigh and Suzuki, respectively, since X is log-normally distributed [16].

The random variables $\{J_p/N_B\}$ are independent identically distributed. If N_B is large enough, then the distribution of $\tilde{J}$ can be approximated with a random variable that has a normal distribution with mean $2\sigma^2$ and variance $4\sigma^4/N_B$. The average coherence bandwidth B_c of CM1–4 are around 32, 16, 11 and 6 MHz, respectively, [17]. With a bandwidth B equal to, e.g., 1500 MHz, the number of blocks N_B becomes 46, 93, 136, and 250 for CM1–4, respectively.

Realizations have different ε_{pb}/N_0. The received power on the IEEE 802.15.3a channel is $P_{r,\text{UWB}} = P_{r,\text{fs}} G_{\text{CIR}}$, which gives $\varepsilon_{pb}/N_0 \approx P_{r,\text{fs}} G_{\text{CIR}} \text{PG}/P_N = P_{r,\text{fs}} X^2 \tilde{J} \text{PG}/P_N$. The expected value of G_{CIR} is given by $\bar{G}_{\text{CIR}} = \text{E}[G_{\text{CIR}}] \approx \text{E}[X^2]\,\text{E}[\tilde{J}] = 10^{\sigma_n^2 \ln(10)/200 + \mu_n/10} 2\sigma^2$. For $\mu_n = 0$, $\sigma_n = 3$, and $2\sigma^2 = 1$, $\bar{G}_{\text{CIR}} \approx 1.27$ (1.04 dB).

If the bandwidth B increases, the performance of a system normally improves due to better diversity combination. In addition, as seen above, the increased bandwidth leads to less variation of G_{CIR} and consequently to less variation of the received power. With, e.g., $N_B = 40$ blocks, J is almost constant. With fewer severe fading dips, the performance is expected to improve. The opposite happens when $B < B_c$, then we can expect that J is exponentially distributed and that the receiver experiences a flat Rayleigh fading channel.

IV. Intrasystem Interference

One method of finding how much intrasystem interference a system can tolerate is to first decide a required PER of, e.g., 8%. Second, the required ε_{pb}/N_0 to achieve this PER without interference is found and is denoted γ_{req}. Then, in presence of interference, a new higher $\varepsilon_{pb}/N_0 = a\gamma_{\text{req}}$ where $a \geqslant 1$ is used. Finally, the minimum required signal-to-interference ratio (SIR) is found that gives the required PER of 8%. An increase of ε_{pb}/N_0 with a gives a decrease of the transmitter–receiver separation with $a^{1/n_{\text{plc}}}$, where n_{plc} is the path loss coefficient. Normal values of $10\log_{10} a$ are 1, 3, and 6 dB which corresponds to a decrease of the distances with a factor of 1.12, 1.41, and 2.0, respectively, for $n_{\text{plc}} = 2$.

The signal-to-interference ratio is given by $\text{SIR} = P_S/P_I$ where the P_S and P_I are the desired signal power and interference power, respectively. If two transmitters have the same transmit power, then $\text{SIR} = P_S/P_I = (d_I/d_S)^{n_{\text{plc}}}$, where d_S and d_I are the distances from the desired transmitter and the interfering transmitter to the receiver, respectively.

Assuming that the contribution of the intrasystem interference after despreading is Gaussian and that it occupies the same RF bandwidth B as the desired signal, the power of the interference is $P_I = I_0 B$, where I_0 is the spectral density of the interference. Assume also that the noise bandwidth, the RF bandwidth, and that the chip rate are all equal, so that $B_N = B = R_c$. With $P_S = \varepsilon_{pb} R_b$, $\text{SIR} = (\varepsilon_{pb}/I_0)/\text{PG}$, where PG is the processing gain. The Gaussian interference assumptions gives that $\varepsilon_{pb}/(N_0 + I_0) = \gamma_{\text{req}}$. Since $(\varepsilon_{pb}/(N_0 + I_0))^{-1} = (\varepsilon_{pb}/N_0)^{-1} + (\varepsilon_{pb}/I_0)^{-1}$, it gives that $1/\gamma_{\text{req}} = 1/(a\gamma_{\text{req}}) + I_0/\varepsilon_{pb}$, which leads to $\varepsilon_{pb}/I_0 = \gamma_{\text{req}}(a/(a-1))$. Thus, the minimum required SIR is given by $\text{SIR} = \gamma_{\text{req}} a/((a-1)\text{PG})$. Clearly, if a better error correcting code is selected so that γ_{req} decreases with a coding gain G_c, then the required SIR drops with G_c. Normally, a higher data rate gives a lower processing gain, a lower coding gain and a higher SIR.

The amount of intrasystem interference P_I that a system can handle depends only on the noise power P_N and a. Since $\varepsilon_{pb}/I_0 = (\varepsilon_{pb}/(N_0 + I_0))(a/(a-1))$ we get $I_0 = N_0(a-1)$ and $P_I = N_0 B(a-1) = P_N(a-1)$.

V. System Parameters

One packet contains $N_i = 8192$ information bits, i.e., 1024 bytes. A square root raised cosine (SRRC) pulse that was truncated at $\pm 6T_c$ with a roll-off factor of 0.2 was used. The arrival time in the receiver of the first path is assumed perfectly known. The implementation loss on the AWGN channel L_I and the noise figure N_F were assumed to be 3 dB and 7 dB, respectively. A decrease in L_I or N_F with θ dB increases the presented transmitter–receiver separation with a factor of $10^{\theta/(10 n_{\text{plc}})}$, where $n_{\text{plc}} = 2$ is the path loss coefficient.

VI. Numerical Results

An IEEE 802.15.3a channel realization $h(t)$ is time invariant during a connection but is completely different between connections. For each of the channel models CM1–CM4, the same 100 channel realizations were used. The presented PER on CM1–CM4 is the 90th-percentile PER, which is denoted PER_{90}. With a 90% probability, the obtained PER during a connection is lower than or equal to the presented PER_{90}. On the AWGN channel, there exists only one PER.

A. Required Chip Rate

After testing several chip rates, it was found that a single-band chip-spaced system with a rake combiner and a sliding window channel estimator is able to give a PER_{90} of 8% with 1024 payload bytes for 110 Mbps at 10 meters on CM4. A chip rate R_c of 1540 Mchip/s and QPSK modulation were used. Further, the carrier frequency f_c is 4.0 GHz, which gives the -10 dB edges $f_{\text{min}} \approx 3.14$ GHz and $f_{\text{max}} \approx 4.86$ GHz.

Three information data rates R_b were investigated, 110 Mbps, 205 Mbps, and 513 Mbps, which correspond to the code rates 1/28, 1/15, and 1/6, respectively. For 110 Mbps, the outer convolutional code has rate 1/7 and the inner repetition code has rate 1/4. 205 Mbps is obtained with an outer code with rate 1/5 and an inner code with rate 1/3. Using only an outer convolutional code with rate 1/6 and no inner code, 513 Mbps is obtained. The constraint length of the convolutional codes are 7.

B. Link Budget on the AWGN Channel

Tab. II shows the link budget for the system on the AWGN channel. Definitions of the parameters can be found in Sec. II-C and the assumptions of N_F and L_I in Sec. V. FCC set the maximum PSD $P_0 = 75$ nW/MHz [1]. Since B is assumed to be equal to R_c, the transmitted power P_t can be shown to be exactly $P_0 R_c$ for the untruncated SRRC pulse. The value of the roll-off factor does not affect P_t. This gives $P_t \approx -9.4$ dBm.

TABLE II

LINK BUDGET FOR THE SINGLE-BAND SYSTEM ON THE AWGN CHANNEL.

Parameter	Value	Value	Value	Unit
Payload bit rate (R_b)	110	205	513	Mbps
Distance (d)	10	4	2	meter
Mean Tx Power (P_t)	-9.4	-9.4	-9.4	dBm
Tx antenna gain (G_t)	0	0	0	dBi
Free-space path loss ($L_p(d)$)	64.3	56.3	50.3	dB
Rx antenna gain (G_r)	0	0	0	dBi
Mean Rx power ($\bar{P}_{r,\text{AWGN}}$)	-73.7	-65.7	-59.7	dBm
Thermal noise power (N_t)	-82.0	-82.0	-82.0	dBm
Rx noise figure (N_F)	7	7	7	dB
Implementation loss (L_I)	3	3	3	dB
Noise power (P_N)	-72.0	-72.0	-72.0	dBm
Processing gain (PG)	11.5	8.8	4.8	dB
SNR per payload bit (ε_{pb}/N_0)	9.8	15.0	17.1	dB
Req. ε_{pb}/N_0 AWGN (Γ_{fs})	3.3	3.5	3.4	dB
Rx sensitivity AWGN (Ψ)	-80.1	-77.2	-73.3	dBm
Link margin (M_L)	6.5	11.5	13.7	dB

Tab. II shows the minimum required ε_{pb}/N_0 on the AWGN channel to give an 8% PER, Γ_{fs}. The values were obtained through simulations. The differences of up to 0.2 dB are due to the different coding gains of the convolutional codes. The Rx sensitivities on the AWGN channel Ψ for 110 Mbps at 10 meters, 205 Mbps at 4 meters, and 513 Mbps at 2 meters are -80.1, -77.2, and -73.3 dBm, respectively. This is the minimum required received power to give a PER of 8% on the AWGN channel. The link margins M_L are 6.5, 11.7, and 14.3 dB for the three rates, respectively.

C. Rake Fingers and Pilots

For the requirement of 110 Mbps at 10 meters, only CM3 and CM4 are considered since they are valid at 10 meters, which CM1 and CM2 are not. It is more difficult to fulfill this requirement on CM4 than on CM3 since CM4 has the largest delay spread, according to Tab. I. As seen in Tab. III, N_p = 16000 pilots are not enough to obtain a PER less than 10% on CM4. A PER around 7% is obtained with 32000 pilots and 60 rake fingers or with 64000 pilots and 55 rake fingers. For CM3, Tab. III shows that 16 fingers with 16000 pilots or 17 fingers with 8000 pilots are enough to obtain an 8% PER.

Note the large difference in the required number of fingers and pilots between CM3 and CM4 for 110 Mbps. Further, the PER decreases slowly with the number of rake fingers on CM4. Thus, the system has clear problems to fulfill the 110 Mbps requirement. The PER decreases much faster with the number of rake fingers on CM3 than on CM4. This gives room for performance improvement by increasing the number of fingers on CM3.

The required number of fingers and pilots for 205 Mbps at 4 meters are presented in Tab. III. Here all four models CM1–4 are valid. With 32000 pilots on CM4, we see that only 12 fingers is needed, which is much less than the 60 fingers for 110 Mbps at 10 meters. Further, with 16000 pilots on CM3, the number of required fingers drops to 7. On CM1, i.e., a line-of-sight model between 1 and 4 meters, 1000 pilots and 3 fingers are enough. Adding more than 1000 pilots on CM1 does not decrease the number of required fingers. Even on CM2, 1000 pilots is enough with 5 fingers. Note the large difference in the required number of fingers and pilots between the different models at 4 meters with 205 Mbps. The system has no problem to fulfill the this requirement since the PER decreases rapidly with the number of rake fingers.

TABLE III

THE NUMBER OF PILOTS AND FINGERS VS. THE 90TH-PERCENTILE PER.

Rate (Mbps)	d (m)	Channel	N_p pilots	N_R fingers	PER_{90}
110	10	CM4	16000	any	$> 10\%$
110	10	CM4	32000	50	10%
110	10	CM4	32000	60	7%
110	10	CM4	32000	70	6%
110	10	CM4	64000	50	9%
110	10	CM4	64000	55	7%
110	10	CM4	64000	60	6%
110	10	CM4	64000	70	4%
110	10	CM3	8000	17	7%
110	10	CM3	16000	16	7%
110	10	CM3	32000	16	6%
205	4	CM4	32000	12	6%
205	4	CM3	8000	7	7%
205	4	CM3	16000	7	5%
205	4	CM3	16000	8	2.5%
205	4	CM2	500	6	2.5%
205	4	CM2	1000	4	12%
205	4	CM2	1000	5	1.7%
205	4	CM2	2000	4	6%
205	4	CM2	4000	4	4%
205	4	CM2	8000	4	3%
205	4	CM1	500	4	4%
205	4	CM1	1000	3	8%
205	4	CM1	1000	4	1.5%
205	4	CM1	2000	3	7%
205	4	CM1	4000	3	5%
205	4	CM1	8000	3	3%

D. Obtained Distances

Tab. IV shows that the system gives a PER of 8% on the AWGN channel at 21 meters for 110 Mbps, 15.1 meters for 205 Mbps, and 9.7 meters for 513 Mbps. As expected, these distances are larger than the required 10, 4, and 2 meters since the link margins M_L in Tab II are positive.

Using 60 rake fingers and 32000 pilots, the system fulfills the requirements of at least 110 Mbps at 10 meters, at least 200 Mbps at 4 meters, and the optional one of at least 480 Mbps at 2 meters. A 90th-percentile PER less than 8% is obtained with 110 Mbps at 10 meters on CM4, 205 Mbps at 6.7 meters

TABLE IV
THE OBTAINED DISTANCES THAT GIVES AN 8% PER.

Rate (Mbps)	d (m)	Channel	Pilots N_p	Fingers N_R	Channel estimator
110	21.0	AWGN	0	1	Perfect
205	15.1	AWGN	0	1	Perfect
513	9.7	AWGN	0	1	Perfect
110	10.0	CM4	32000	60	SW
110	13.2	CM3	32000	60	SW
205	6.7	CM4	32000	60	SW
205	8.6	CM3	32000	60	SW
513	3.8	CM2	32000	60	SW
110	7.4	CM4	16000	16	SW
110	10.0	CM3	16000	16	SW
205	4.5	CM4	16000	16	SW
205	6.2	CM3	16000	16	SW
513	2.9	CM2	16000	16	SW

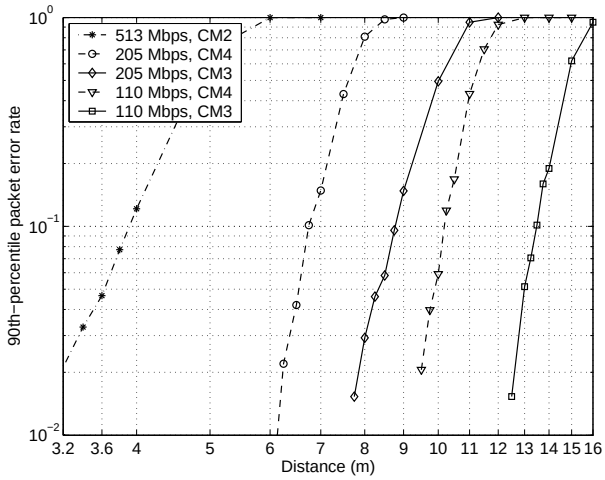

Fig. 2. The 90th-percentile PER vs. distance with $N_R = 60$ rake fingers and $N_p = 32000$ pilots for 110, 205, and 513 Mbps.

on CM4, and 513 Mbps at 3.8 meters at CM2. For details, please see Tab. IV and Fig. 2. Since this setup fulfills all the requirements, it shows that the link margins M_L in Tab. II are sufficient.

If the requirement is relaxed so that only 110 Mbps at 10 meters is obtained on CM3 but not on CM4, the number of fingers can be reduced to 16 using only 16000 pilots, according to Tab. IV. Then only 7.4 meters is obtained on CM4 for 110 Mbps. However, this second setup gives 4.5 meters for 205 Mbps on CM4 and 2.9 meters for 513 Mbps on CM2, and thus this setup fulfills two out of three requirements.

VII. CONCLUSIONS

The investigated single-band system with a chip rate of 1540 Mchip/s can provide a payload bit rate of 110 Mbps at 10 meters on CM4, 205 Mbps at 6.7 meters on CM4, and 513 Mbps at 3.8 meters on CM2, which fulfills the requirements from IEEE 802.15.3a. At those distances, the 90th-percentile PER is 8% with 1024 payload bytes. A chip-spaced rake combiner with a sliding window (SW) channel estimator, 60 rake fingers, and 32000 pilots was used. The system has clear problems to fulfill the 110 Mbps at 10 meter requirement on CM4, since the PER decreases slowly with the number of rake fingers. This is not the case on CM1–3. It might not be feasible to have 60 rake fingers using normal methods. However, using, e.g., overlap-add FFT filtering could give lower complexity. Further, 16 rake fingers gives 110 Mbps at 10 meters on CM3. A designer issue is then how probable the 10 meter scenario on CM4 is.

ACKNOWLEDGMENT

This work has been funded by Ultrawaves, PCC++, and the Swedish Research Council. The authors would like to express their gratitude to the partners in Ultrawaves for sharing their expertise in UWB systems.

REFERENCES

[1] "Revision of part 15 of the commission's rules regarding ultra-wideband transmission systems," Federal Communications Commission, First Report and Order, ET Docket 98–153, Apr. 2002.

[2] A. Batra et al., "TI physical layer proposal for IEEE 802.15 task group 3a," Doc. no. P802.15-03/142r1-TG3a, IEEE P802.15 WPAN, May 2003, available at http://grouper.ieee.org/groups/802/15/.

[3] A. Batra et al., "Multi-band OFDM physical layer proposal for IEEE 802.15.3a," Sept. 2004, available at http://www.multibandofdm.org.

[4] R. Roberts, "XtremeSpectrum CFP document," Doc. no. P802.15-03/154r3, IEEE P802.15 WPAN, July 2003, available at http://grouper.ieee.org/groups/802/15/.

[5] R. Fisher et al., "DS-UWB physical layer submission to 802.15 task group 3a," Doc. no. P802.15-04/137r3, IEEE P802.15 WPAN, July 2004, available at http://grouper.ieee.org/groups/802/15/.

[6] J. Foerster et al., "Channel modeling sub-committee report final," Doc. no. P802.15-02/490r1-SG3a, IEEE P802.15 WPAN, Feb. 2003, available at http://grouper.ieee.org/groups/802/15/.

[7] A. Saleh and R. Valenzuela, "A statistical model for indoor multipath propagation," *IEEE Journal on Select. Areas Commun.*, vol. 5, pp. 128–137, Feb. 1987.

[8] M.-O. Wessman, ed., "D4.1: Transceiver study and preliminary design report," Doc. no. W04-03-0017-P04, Ultrawaves, Apr. 2003, available at http://www.ultrawaves.org.

[9] B. Mielczarek, M.-O. Wessman, and A. Svensson, "Performance of coherent UWB rake receivers with channel estimators," *IEEE VTC'03 fall*, Orlando, FL, USA, Oct. 2003.

[10] M.-O. Wessman et al., "D4.2: Transceiver design and link level simulation results," Doc. no. W04-03-0025-R07, Ultrawaves, Dec. 2003, available at http://www.ultrawaves.org.

[11] M.-O. Wessman et al., "D4.2: Transceiver design and link level simulation results - part II, rev II," Doc. no. W04-03-0025-R14, Ultrawaves, Dec. 2004, available at http://www.ultrawaves.org.

[12] J. Ellis et al., "P802.15.TG3a alt PHY selection criteria," Doc. no. P802.15-03/031r11, IEEE P802.15 WPAN, May 2003, available at http://grouper.ieee.org/groups/802/15/.

[13] J. Ellis et al., "TG3a technical requirements," Doc. no. P802.15-03/030r0, IEEE P802.15 WPAN, Dec. 2002, available at http://grouper.ieee.org/groups/802/15/.

[14] M.-O. Wessman, A. Svensson, and E. Agrell, "Design and performance of carrier-based direct-sequence ultra-wideband systems," Doc. no. R013/2005, Dept. of Signal and Systems, Chalmers Univ. of Tech., Apr. 2005, available at http://www.s2.chalmers.se/publications/.

[15] G. R. Grimmett and D. R. Stirzaker, *Probability and random processes,* Oxford University Press, 3rd ed., 2001.

[16] H. Suzuki, "A statistical model for urban radio propagation," *IEEE Trans on Comm.*, vol. 25, no. 7, pp. 673–680, July 1977.

[17] M.-O. Wessman, A. Svensson and E. Agrell, "Frequency diversity performance of coded multiband-OFDM systems on IEEE UWB Channels," *IEEE VTC'04 fall*, Los Angeles, CA, USA, Sept. 2004.